Acta Crystallographica Section C
Crystal Structure Communications
ISSN 0108-2701

Polarized molecular–electronic structures and supramolecular aggregation in 1-(6-amino-1,3-benzodioxol-5-yl)-3-arylprop-2-en-1-ones

John N. Low,[a] Justo Cobo,[b] Manuel Nogueras,[b] Paola Cuervo,[c] Rodrigo Abonia[c] and Christopher Glidewell[d]*

[a]Department of Chemistry, University of Aberdeen, Meston Walk, Old Aberdeen AB24 3UE, Scotland, [b]Departamento de Química Inorgánica y Orgánica, Universidad de Jaén, 23071 Jaén, Spain, [c]Grupo de Investigación de Compuestos Heterocíclicos, Departamento de Química, Universidad de Valle, AA 25360 Cali, Colombia, and [d]School of Chemistry, University of St Andrews, Fife KY16 9ST, Scotland
Correspondence e-mail: cg@st-andrews.ac.uk

Received 12 August 2004
Accepted 16 August 2004
Online 18 September 2004

Molecules of 1-(6-amino-1,3-benzodioxol-5-yl)-3-(4-methylphenyl)prop-2-en-1-one, $C_{17}H_{15}NO_3$, (I), 1-(6-amino-1,3-benzodioxol-5-yl)-3-(4-methoxyphenyl)prop-2-en-1-one, $C_{17}H_{15}NO_4$, (II), and 1-(6-amino-1,3-benzodioxol-5-yl)-3-[4-(trifluoromethyl)phenyl]prop-2-en-1-one, $C_{17}H_{12}F_3NO_3$, (III), all contain an intramolecular N—H···O hydrogen bond and all exhibit polarized molecular–electronic structures. The molecules of (I) are linked into simple sheets, generated by translation, by means of one N—H···O and one C—H···π(arene) hydrogen bond. Compound (II) crystallizes as two concomitant polymorphs, *viz*. (II*a*), with $Z' = 1$ in $P2_1/c$, and (II*b*), with $Z' = 2$ in $P\overline{1}$. In (II*a*), intra- and intermolecular N—H···O hydrogen bonds generate a helical chain of rings, and these chains are linked into sheets by simple helical chains built from a C—H···π(arene) hydrogen bond, while in (II*b*), the molecules are linked into simple chains by a C—H···O hydrogen bond. In (III), where $Z' = 2$, each type of molecule forms a simple N—H···O hydrogen-bonded chain generated by translation and the two types of chain are linked by a single π–π stacking interaction.

Comment

A range of 2-aminochalcone derivatives have been prepared for use as intermediates in the synthesis of new 6,7-methylenedioxytetrahydroquinolin-4-ones, compounds with interesting biological and pharmacological properties (Donnelly & Farell, 1990; Prager & Thredgold, 1968; Kurasawa *et al.*, 2002). We report here the molecular and supramolecular structures of three such compounds, (I)–(III), and compare them with two further examples, (IV) and (V) (Low *et al.*, 2002).

Compounds (I) and (III) crystallize with Z' values of 1 and 2, respectively, while compound (II) forms two polymorphs, *viz*. monoclinic and triclinic, denoted (II*a*) and (II*b*), respectively, which crystallize concomitantly from dimethylformamide, with Z' values of 1 and 2, respectively (Figs. 1–4). Of the two polymorphs of (II), the monoclinic polymorph has a significantly higher density than the triclinic polymorph and hence is probably the thermodynamically more stable form (Burger & Ramberger, 1979).

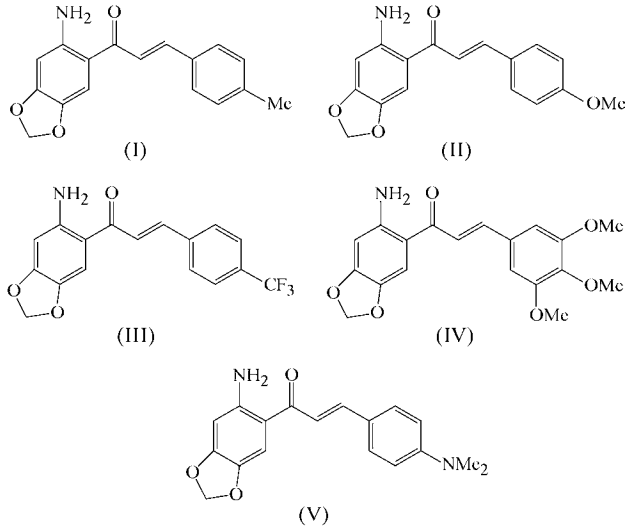

(I) (II) (III) (IV) (V)

There is significant bond fixation within the amino-substituted aryl rings of (I)–(III) (Table 1). In particular, the C3a—C4 and C7—C7a bonds are both short, while the C5—C6 and C6—C7 bonds are long. In addition, the C6—C8 bond is short for its type (mean value 1.488 Å; Allen *et al.*, 1987), while C8—O8 is long (mean value 1.231 Å). These values point to the charge-separated form, (*A*) (see scheme below), as an important contributor to the overall molecular–electronic structure, alongside the delocalized form, (*B*). An entirely similar pattern of distances (Table 1) is observed in the analogous compounds (IV) and (V), the structures of which have recently been reported (Low *et al.*, 2002), although this was not discussed or noted in the original report, which focused exclusively on the supramolecular aggregation of (IV) and (V).

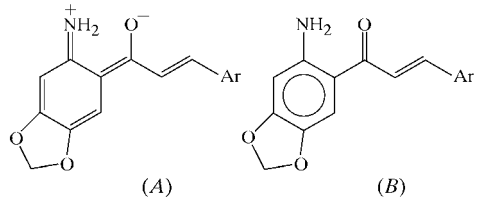

(*A*) (*B*)

In all cases, the molecular skeletons are fairly close to being planar but, as shown by the key torsion angles (Table 2), there are some significant deviations in most of the independent examples. The sole exception is the type 1 molecule (containing atom O11, *etc*.; Fig. 3*a*) of compound (III). The five-membered rings show some flexibility of conformational behaviour. Thus, this ring is planar in (II*a*) [although not in (II*b*)] and in the type 2 molecule of compound (III), but it

  DOI: 10.1107/S0108270104020414

adopts an envelope conformation, with a folding across the O···O line, in (I), in both molecules of (II*b*) and in the type 1 molecule of (III). For these rings, the ring-puckering parameter φ_2 (Cremer & Pople, 1975) takes the values 31.1 (15) and 30.5 (9)° in (I) and (III), respectively, and 30.9 (5) and 213.7 (5)° in the two independent molecules of (II*b*). The two independent molecules in (II*b*) exhibit different conformations at the methoxy substituent (Table 2), and this alone is sufficient to preclude the possibility of any additional symmetry

All of the molecules contain an intramolecular N—H···O hydrogen bond (Tables 3–6), in each case generating an *S*(6) motif (Bernstein *et al.*, 1995), and these may have some influence on the overall molecular conformations. The supramolecular structures of (I) and (II*a*) both depend upon a combination of N—H···O and C—H···π(arene) hydrogen bonds to generate sheets, but the structures differ considerably in detail. In compound (I), the amine atom N5 in the molecule at (*x*, *y*, *z*) acts as hydrogen-bond donor, *via* atom H5*B*, to ring atom O1 in the molecule at (*x*, *y* − 1, *z*), so generating by translation a *C*(7) chain running parallel to the

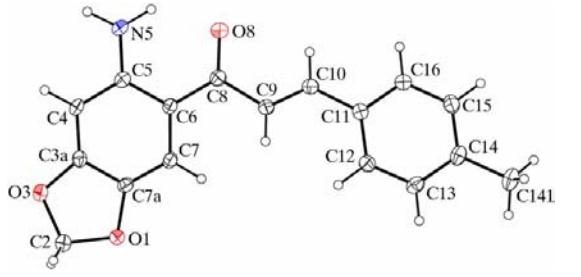

Figure 1
The molecule of (I), showing the atom-labelling scheme. Displacement ellipsoids are drawn at the 30% probability level and H atoms are shown as small spheres of arbitrary radii.

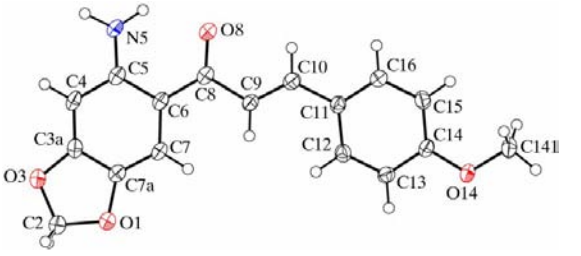

Figure 2
The molecule of (II*a*), showing the atom-labelling scheme. Displacement ellipsoids are drawn at the 30% probability level and H atoms are shown as small spheres of arbitrary radii.

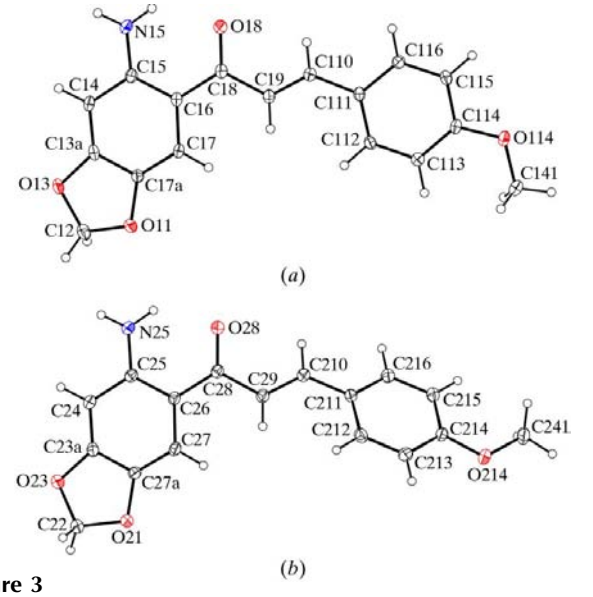

Figure 3
The two independent molecules of (II*b*), showing the atom-labelling scheme for (*a*) the type 1 molecule and (*b*) the type 2 molecule. Displacement ellipsoids are drawn at the 30% probability level and H atoms are shown as small spheres of arbitrary radii.

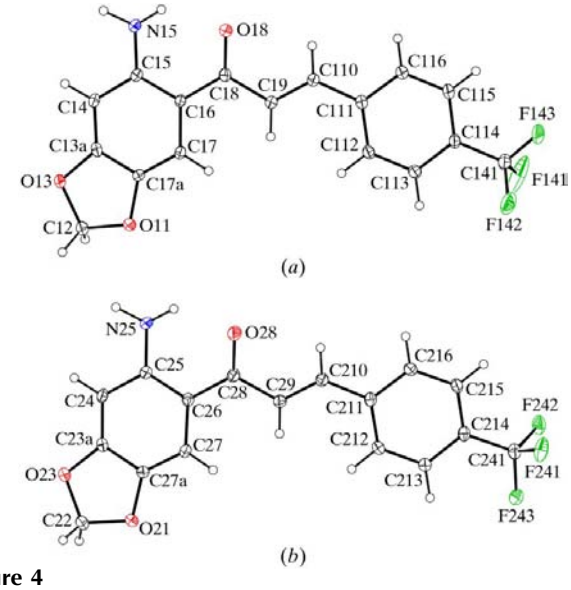

Figure 4
The two independent molecules of (III), showing the atom-labelling scheme for (*a*) the type 1 molecule and (*b*) the type 2 molecule. Displacement ellipsoids are drawn at the 30% probability level and H atoms are shown as small spheres of arbitrary radii.

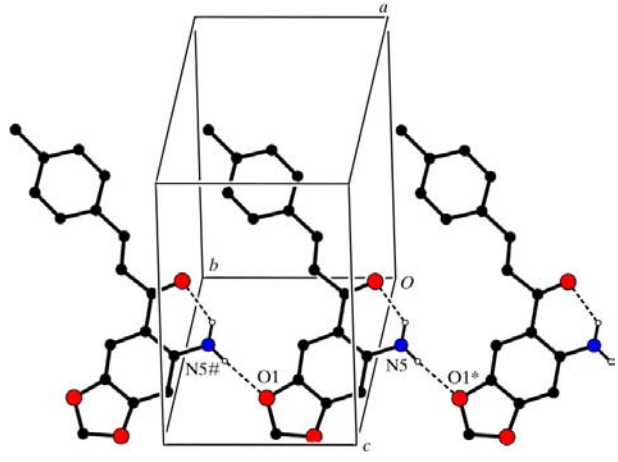

Figure 5
Part of the crystal structure of (I), showing the formation of a chain parallel to [010]. For the sake of clarity, H atoms bonded to C atoms have been omitted. Atoms marked with an asterisk (*) or a hash (#) are at the symmetry positions (*x*, *y* − 1, *z*) and (*x*, 1 + *y*, *z*), respectively.

[010] direction (Fig. 5). In addition, atom C2 in the molecule at (x, y, z) acts as hydrogen-bond donor, *via* atom H2*A*, to the C11–C16 ring in the molecule at ($x-1$, y, z), so generating by translation a chain running parallel to the [100] direction (Fig. 6). The combination of the [100] and [010] chains generates a sheet parallel to (001), lying in the domain $\frac{1}{2} < z < \frac{3}{4}$ (Fig. 7). Four sheets of this type pass through each unit cell, but there are no direction-specific interactions between adjacent sheets.

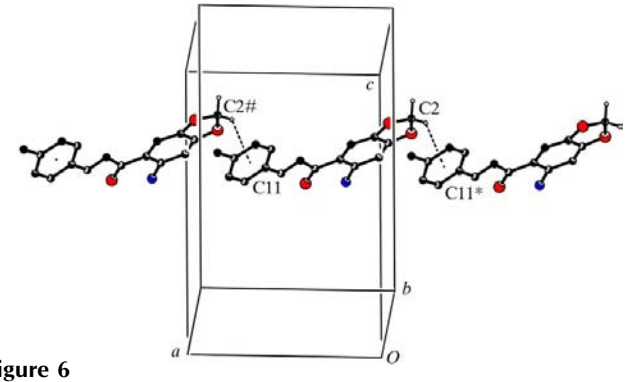

Figure 6
Part of the crystal structure of (I), showing the formation of a chain parallel to [100]. For the sake of clarity, H atoms bonded to C atoms not involved in the motif shown have been omitted. Atoms marked with an asterisk (*) or a hash (#) are at the symmetry positions ($x-1$, y, z) and ($1+x$, y, z), respectively.

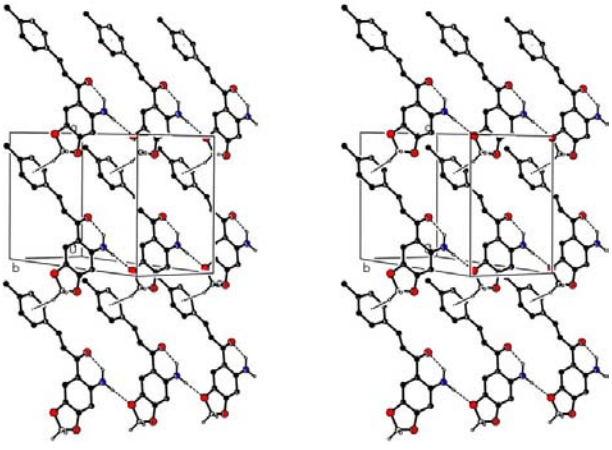

Figure 7
A stereoview of part of the crystal structure of (I), showing the formation of a sheet parallel to (001). For the sake of clarity, H atoms bonded to C atoms not involved in the motif shown have been omitted.

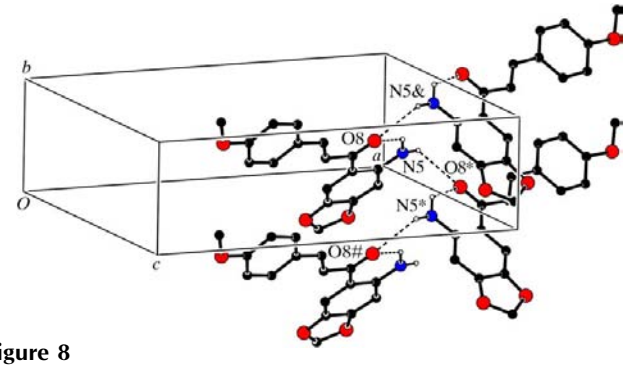

Figure 8
Part of the crystal structure of polymorph (II*a*), showing the formation of a chain of rings parallel to [010]. For the sake of clarity, H atoms bonded to C atoms have been omitted. Atoms marked with an asterisk (*), a hash (#) or an ampersand (&) are at the symmetry positions ($2-x$, $y-\frac{1}{2}$, $\frac{1}{2}-z$), (x, $y-1$, z) and ($2-x$, $\frac{1}{2}+y$, $\frac{1}{2}-z$), respectively.

The monoclinic polymorph (II*a*) of compound (II) exhibits two C—H$\cdots\pi$(arene) hydrogen bonds in addition to the two N—H$\cdots$O interactions (Table 4). Amine atom N5 in the molecule at (x, y, z) acts as donor, again *via* atom H5*B*, but this time to carbonyl atom O8 in the molecule at ($2-x$, $y-\frac{1}{2}$, $\frac{1}{2}-z$), so producing a helical $C_2^1(4)C(6)[S(6)]$ chain of rings running parallel to the [010] direction and generated by the 2_1 screw axis along (1, y, $\frac{1}{4}$) (Fig. 8). This chain of rings may be contrasted with the very simple chain formed by the N—H$\cdots$O hydrogen bonds in compound (I) (Fig. 5). Of the two C—H$\cdots\pi$(arene) hydrogen bonds, that having atom C2 as the donor simply reinforces the foregoing [010] chain. However, that involving atom C13 in the molecule at (x, y, z) as donor to

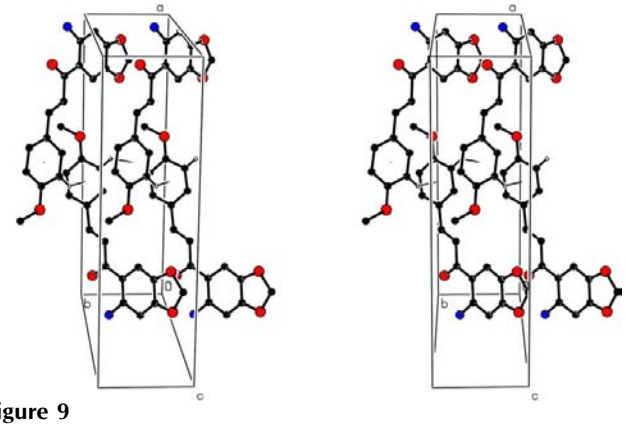

Figure 9
A stereoview of part of the crystal structure of polymorph (II*a*), showing the formation of an [010] chain generated by C—H$\cdots\pi$(arene) hydrogen bonds. For the sake of clarity, H atoms not involved in the motif shown have been omitted.

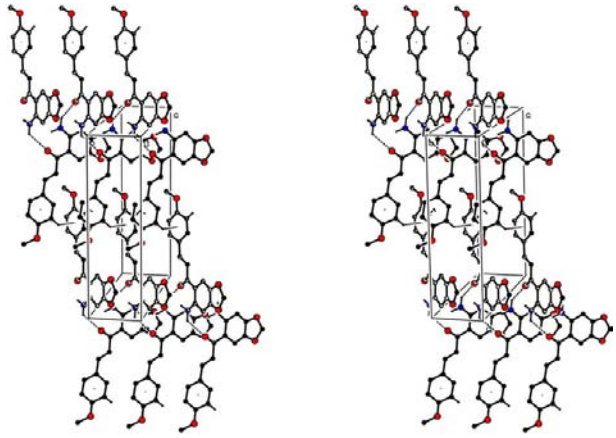

Figure 10
A stereoview of part of the crystal structure of polymorph (II*a*), showing the formation of a sheet parallel to (001). For the sake of clarity, the intramolecular hydrogen bond and H atoms bonded to C atoms and not involved in the motif shown have been omitted.

the C11–C16 ring in the molecule at $(1-x, y-\frac{1}{2}, \frac{1}{2}-z)$ not only generates a second chain running parallel to [010], this time generated by the 2_1 axis along $(\frac{1}{2}, y, \frac{1}{4})$ (Fig. 9), but also serves to link all of the chain of rings into an (001) sheet (Fig. 10). In the triclinic polymorph (II*b*), the type 1 molecules (Fig. 3*a*) are linked by means of a single C—H···O hydrogen bond into chains generated by translation, while the type 2 molecules (Fig. 3*b*) are pendent from these chains and linked to them by N—H···O hydrogen bonds (Fig. 11)

Each of the two independent molecules in compound (III) forms a simple *C*(7) chain. The amine atoms N15 and N25 in the molecules at (x, y, z) act as donors to, respectively, the ring atoms O11 and O21 in the molecules at $(x-1, y, z)$, so generating *C*(7) chains by translation (Table 5 and Fig. 12). These two chains are linked by an aromatic π–π stacking interaction between the C111–C116 and C211–C216 rings within the asymmetric unit. The dihedral angle between the planes of these two rings is only 4.5 (2)°, the interplanar spacing is *ca* 3.5 Å and the centroid–centroid separation is 3.618 (2) Å. Propagation of this interaction then links the two independent translational chains (Fig. 12)

The simple and complex sheets in (I) and (II*a*), the single chains in (II*b*) and the paired chains in (III) may be briefly compared with the supramolecular structures of the analogues (IV) and (V) (Low *et al.*, 2002). In (IV), where $Z' = 1$, the sole significant intermolecular interactions are a C—H···O hydrogen bond with a ring O atom as acceptor, which generates zigzag *C*(10) chains, and a π–π stacking interaction linking these chains into sheets. In (V), where $Z' = 2$, two N—H···O hydrogen bonds generate centrosymmetric $R_8^4(16)$ tetramers, which are weakly linked into chains by two rather long C—H···O hydrogen bonds. Hence, for the five compounds (I)–(V), while their intramolecular properties are all very similar, their supramolecular aggregation patterns are all different. For no single example in this series could the supramolecular structure be predicted from a knowledge of the supramolecular structures of all the others.

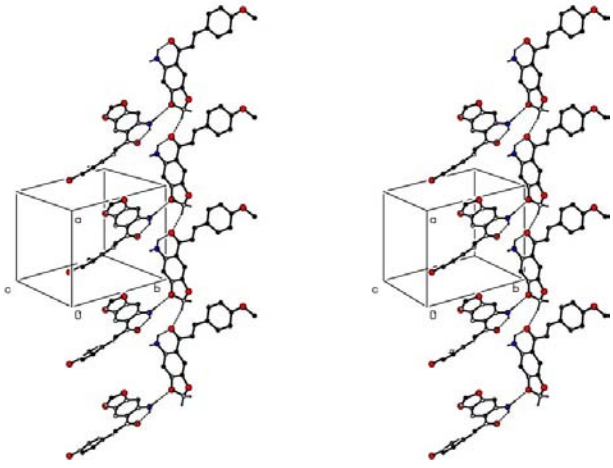

Figure 11
A stereoview of part of the crystal structure of polymorph (II*b*), showing the formation of a *C*(8) chain along [100]. For the sake of clarity, the intramolecular hydrogen bond and H atoms bonded to C atoms and not involved in the motif shown have been omitted.

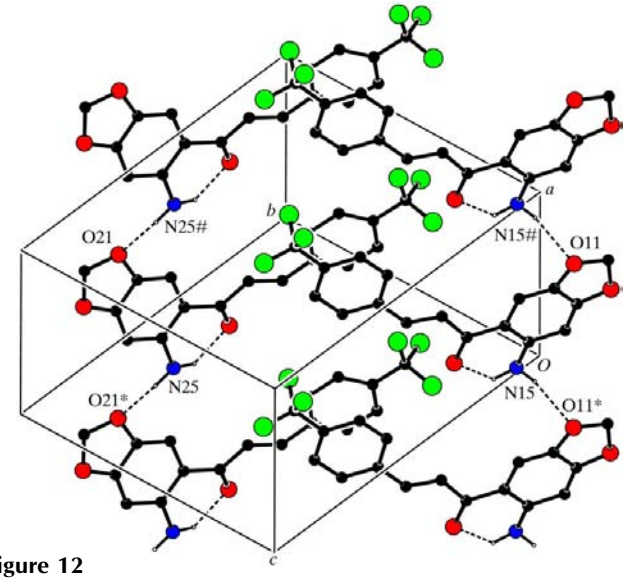

Figure 12
Part of the crystal structure of (III), showing the formation of a π-stacked pair of chains parallel to [100]. For the sake of clarity, H atoms bonded to C atoms have been omitted. Atoms marked with an asterisk (*) or a hash (#) are at the symmetry positions $(x-1, y, z)$ and $(1+x, y, z)$, respectively.

Experimental

For the synthesis of (I), a solution of 6-amino-3,4-methylenedioxyacetophenone (0.5 g, 2.79 mmol), 4-tolualdehyde (0.33 g, 2.75 mmol), ethanol (10 ml) and aqueous NaOH (0.5 ml, 20%) was heated under reflux for 20 min. After cooling the mixture, the resulting precipitate was filtered off and washed with ethanol, yielding (I) as a yellow solid (yield 91%, m.p. 401 K). Spectroscopic analysis, IR (KBr disc, ν, cm^{-1}): 3454, 3278 (NH_2), 1646 (C═O), 1606 (C═C), 1224 (OCH_2O); ^{1}H NMR (DMSO-d_6, δ): 2.33 (3H, *s*, CH_3), 5.96 (2H, *s*, OCH_2O), 6.35 (1H, *s*), 7.23 (2H, *d*, J = 8.0 Hz), 7.53 (1H, *d*, J = 15.4 Hz), 7.65 (1H, *s*), 7.67 (2H, *br s*, NH_2), 7.73 (2H, *d*, J = 8.0 Hz), 7.81 (1H, *d*, J = 15.4 Hz); ^{13}C NMR (DMSO-d_6, δ): 21.0 (CH_3), 95.8, 101.1 (OCH_2O), 108.0, 109.9, 122.7, 128.5, 129.4, 132.5, 137.7, 139.6, 141.0, 151.7, 152.7, 187.7 (C═O). MS (70 eV): *m*/e (%) 281 (41, [M^+]), 190 (100, [M–C_7H_7]). Crystals of (I) suitable for single-crystal X-ray diffraction were grown from a solution in ethanol. For the synthesis of (II), a solution of 6-amino-3,4-methylenedioxyacetophenone (0.5 g, 2.79 mmol), 4-methoxybenzaldehyde (0.38 g, 2.79 mmol), ethanol (10 ml) and aqueous NaOH (0.5 ml, 20%) was heated under reflux for 30 min. After cooling the mixture, the resulting precipitate was filtered off and crystallized from ethanol, giving (II) as an orange solid (yield 50%, m.p. 405 K). Spectroscopic analysis, IR (KBr disc, ν, cm^{-1}): 3461, 3303 (NH_2), 1644 (C═O), 1603 (C═C), 1223 (OCH_2O); ^{1}H NMR ($CDCl_3$, δ): 3.89 (3H, *s*, OCH_3), 5.93 (2H, *s*, OCH_2O), 6.19 (1H, *s*), 6.57 (2H, *br s*, NH_2), 6.91 (2H, *d*, J = 8.0 Hz), 7.26 (1H, *s*), 7.35 (1H, *d*, J = 15.4 Hz), 7.47 (2H, *d*, J = 8.0 Hz), 7.71 (1H, *d*, J = 15.4 Hz); ^{13}C NMR ($CDCl_3$, δ): 55.2 (OCH_3), 96.8, l01.5 (OCH_2O), 108.2, 112.0, 114.5, 121.2, 128.3, 130.0, 138.9, 142.1, 150.0, 153.5, 161.2, 189.0 (C═O). MS (70 eV): *m*/e (%) 297 (27, [M^+]), 190 (100, [M–C_7H_7O]). Crystallization from dimethylformamide gave a mixture of the monoclinic polymorph (II*a*) as red crystals (m.p. 382 K) and the triclinic polymorph (II*b*) as yellow crystals (m.p. 389 K). For the

Table 1
Selected bond distances (Å) for compounds (I)–(V).

Bond	(I)	(II*a*)	(II*b*) Mol 1	(II*b*) Mol 2	(III) Mol 1	(III) Mol 2	(IV)	(V) Mol 1	(V) Mol 2
x	nil	nil	1	2	1	2	nil	1	2
C*x*3a—C*x*4	1.368 (3)	1.357 (2)	1.357 (2)	1.359 (2)	1.358 (3)	1.355 (3)	1.361 (2)	1.358 (2)	1.351 (2)
C*x*4—C*x*5	1.402 (3)	1.416 (2)	1.418 (2)	1.418 (2)	1.415 (3)	1.417 (3)	1.417 (2)	1.419 (2)	1.418 (2)
C*x*5—C*x*6	1.424 (3)	1.430 (2)	1.423 (2)	1.422 (2)	1.429 (3)	1.419 (3)	1.426 (2)	1.426 (2)	1.431 (2)
C*x*6—C*x*7	1.428 (3)	1.430 (2)	1.420 (2)	1.435 (2)	1.428 (3)	1.421 (3)	1.428 (2)	1.426 (2)	1.423 (2)
C*x*7—C*x*7a	1.339 (3)	1.354 (2)	1.353 (2)	1.350 (2)	1.350 (3)	1.355 (3)	1.355 (2)	1.354 (2)	1.353 (2)
C*x*7a—C*x*3a	1.386 (3)	1.394 (2)	1.387 (2)	1.391 (2)	1.390 (3)	1.390 (3)	1.394 (2)	1.390 (2)	1.393 (2)
C*x*5—N*x*5	1.364 (3)	1.353 (2)	1.364 (2)	1.361 (2)	1.368 (2)	1.369 (3)	1.359 (2)	1.370 (2)	1.360 (2)
C*x*6—C*x*8	1.459 (3)	1.461 (2)	1.470 (2)	1.462 (2)	1.468 (2)	1.468 (3)	1.470 (2)	1.473 (2)	1.463 (2)
C*x*8-O*x*8	1.249 (3)	1.246 (2)	1.240 (2)	1.244 (2)	1.244 (4)	1.237 (2)	1.243 (2)	1.253 (2)	1.250 (2)

Table 2
Selected torsion angles (°) for compounds (I)–(III).

Parameter	(I)	(II*a*)	(II*b*) Mol 1	(II*b*) Mol 2	(III) Mol 1	(III) Mol 2
x	nil	nil	1	2	1	2
C*x*5—C*x*6—C*x*8—C*x*9	−177.8 (2)	179.63 (13)	−168.15 (13)	−175.23 (13)	−171.93 (18)	−156.36 (19)
C*x*6—C*x*8—C*x*9—C*x*10	−159.1 (2)	−175.03 (14)	−170.48 (13)	153.13 (14)	171.9 (2)	176.7 (2)
C*x*8—C*x*9—C*x*10—C*x*11	178.4 (2)	179.77 (14)	−178.12 (13)	−176.05 (13)	−177.59 (19)	−177.65 (19)
C*x*9—C*x*10—C*x*11—C*x*12	−9.0 (2)	5.1 (2)	−11.3 (2)	−16.8 (2)	0.7 (3)	−8.6 (3)
C*x*13—C*x*14—O*x*14—C*x*41		−175.91 (13)	1.4 (2)	−176.09 (14)		

synthesis of (III), a solution of 6-amino-3,4-methylenedioxyacetophenone (0.5 g, 2.79 mmol), 4-(trifluoromethyl)benzaldehyde (0.49 g, 2.79 mmol), ethanol (10 ml) and aqueous NaOH (0.5 ml, 20%) was heated under reflux for 25 min. After cooling the mixture, the resulting precipitate was filtered off and washed with ethanol, yielding (III) as an orange solid (yield 75%, m.p. 417 K). Spectroscopic analysis, IR (KBr disc, ν, cm^{-1}): 3468, 3305 (NH_2), 1646 (C═O), 1606 (C═C), 1228 (OCH_2O); ^{1}H NMR (DMSO-d_6, δ): 5.94 (1H, *s*, H2), 5.98 (2H, *s*, OCH_2O), 6.38 (1H, *s*, H6), 7.6 (1H, *d*, H8, J = 15.0 Hz), 7.69 (2H, *br s*, NH_2), 7.76 (2H, *d*, J = 8.0 Hz), 8.02 (1H, *d*, J = 15.4 Hz), 8.15 (2H, *d*, J = 8.0 Hz); ^{13}C NMR (DMSO-d_6, δ): 95.8, 101.2 (OCH_2O), 108.0, 108.9, 113.5 (CF_3), 125.5, 126.7, 129.3, 138.0, 139.1, 139.4, 152.2, 153.2, 187.1 (C═O). MS (70 eV): *m*/e (%) 335 (100, [M^+]). Crystals of (III) suitable for single-crystal X-ray diffraction were grown from a solution in ethanol.

Compound (I)

Crystal data

$C_{17}H_{15}NO_3$
M_r = 281.30
Monoclinic, $P2_1/n$
a = 10.530 (5) Å
b = 7.362 (5) Å
c = 17.546 (5) Å
β = 91.719 (5)°
V = 1359.6 (12) Å^3
Z = 4
D_x = 1.374 Mg m^{-3}
Mo $K\alpha$ radiation
Cell parameters from 3062 reflections
θ = 5.3–27.5°
μ = 0.10 mm^{-1}
T = 120 (2) K
Block, yellow
0.40 × 0.30 × 0.20 mm

Data collection

Nonius KappaCCD area-detector diffractometer
φ scans, and ω scans with κ offsets
Absorption correction: multi-scan (*EvalCCD*; Duisenberg *et al.*, 2003)
T_{min} = 0.958, T_{max} = 0.981
17 073 measured reflections
3062 independent reflections
2024 reflections with $I > 2\sigma(I)$
R_{int} = 0.065
θ_{max} = 27.5°
$h = -13 \rightarrow 12$
$k = -9 \rightarrow 9$
$l = -22 \rightarrow 22$

Refinement

Refinement on F^2
$R[F^2 > 2\sigma(F^2)]$ = 0.061
$wR(F^2)$ = 0.135
S = 1.11
3062 reflections
191 parameters
H-atom parameters constrained
$w = 1/[\sigma^2(F_o^2) + (0.0198P)^2 + 1.4934P]$ where $P = (F_o^2 + 2F_c^2)/3$
$(\Delta/\sigma)_{max} < 0.001$
$\Delta\rho_{max}$ = 0.24 e Å^{-3}
$\Delta\rho_{min}$ = −0.21 e Å^{-3}

Table 3
Hydrogen-bonding geometry (Å, °) for (I).

*Cg*1 is the centroid of the C11–C16 ring.

D—H···*A*	*D*—H	H···*A*	*D*···*A*	*D*—H···*A*
N5—H5*A*···O8	0.96	1.88	2.612 (3)	131
N5—H5*B*···O1^{i}	0.96	2.07	3.032 (3)	178
C2—H2*A*···*Cg*1^{ii}	0.99	2.86	3.644 (4)	137

Symmetry codes: (i) $x, y-1, z$; (ii) $x-1, y, z$.

Polymorph (II*a*)

Crystal data

$C_{17}H_{15}NO_4$
M_r = 297.30
Monoclinic, $P2_1/c$
a = 17.5560 (4) Å
b = 5.0914 (2) Å
c = 15.4869 (4) Å
β = 91.9240 (16)°
V = 1383.51 (7) Å^3
Z = 4
D_x = 1.427 Mg m^{-3}
Mo $K\alpha$ radiation
Cell parameters from 3170 reflections
θ = 2.9–27.5°
μ = 0.10 mm^{-1}
T = 120 (2) K
Block, red
0.04 × 0.02 × 0.02 mm

Data collection

Nonius KappaCCD area-detector diffractometer
φ and ω scans
Absorption correction: multi-scan (*SADABS*; Sheldrick, 2003)
T_{min} = 0.959, T_{max} = 0.998
14 325 measured reflections
3170 independent reflections
2271 reflections with $I > 2\sigma(I)$
R_{int} = 0.038
θ_{max} = 27.5°
$h = -21 \rightarrow 22$
$k = -6 \rightarrow 6$
$l = -20 \rightarrow 19$

Refinement

Refinement on F^2	$w = 1/[\sigma^2(F_o^2) + (0.0701P)^2 + 0.2374P]$ where $P = (F_o^2 + 2F_c^2)/3$
$R[F^2 > 2\sigma(F^2)] = 0.045$	$(\Delta/\sigma)_{max} = 0.002$
$wR(F^2) = 0.128$	$\Delta\rho_{max} = 0.26$ e Å^{-3}
$S = 1.04$	$\Delta\rho_{min} = -0.21$ e Å^{-3}
3169 reflections	Extinction correction: *SHELXL*97 (Sheldrick, 1997)
201 parameters	Extinction coefficient: 0.007 (2)
H-atom parameters constrained	

Table 4
Hydrogen-bonding geometry (Å, °) for polymorph (II*a*).

*Cg*1 is the centroid of the C11–C16 ring and *Cg*2 is the centroid of the C3a/C4–C7/C7a ring.

D—H···A	D—H	H···A	D···A	D—H···A
N5—H5*A*···O8	0.96	1.95	2.6301 (15)	126
N5—H5*B*···O8^{i}	0.96	2.49	3.1232 (15)	123
C2—H2*B*···*Cg*2^{ii}	0.99	2.84	3.640 (2)	138
C13—H13···*Cg*1^{iii}	0.95	2.81	3.488 (2)	130

Symmetry codes: (i) $2-x, y-\frac{1}{2}, \frac{1}{2}-z$; (ii) $x, y-1, z$; (iii) $1-x, y-\frac{1}{2}, \frac{1}{2}-z$.

Polymorph (II*b*)

Crystal data

$C_{17}H_{15}NO_4$	Mo $K\alpha$ radiation
$M_r = 297.30$	Cell parameters from 6517 reflections
Triclinic, $P\overline{1}$	$\theta = 3.1$–$27.5°$
$a = 9.5352$ (2) Å	$\mu = 0.10$ mm^{-1}
$b = 10.6193$ (3) Å	$T = 120$ (2) K
$c = 14.7611$ (4) Å	Block, yellow
$\alpha = 89.1400$ (14)°	0.45 × 0.30 × 0.20 mm
$\beta = 81.0970$ (17)°	
$\gamma = 75.7540$ (14)°	
$V = 1430.83$ (6) Å^3	
$Z = 4$	
$D_x = 1.380$ Mg m^{-3}	

Data collection

Nonius KappaCCD area-detector diffractometer	4940 reflections with $I > 2\sigma(I)$
φ and ω scans	$R_{int} = 0.035$
Absorption correction: multi-scan (*SADABS*; Sheldrick, 2003)	$\theta_{max} = 27.5°$
$T_{min} = 0.951$, $T_{max} = 0.981$	$h = -12 \rightarrow 12$
23 999 measured reflections	$k = -13 \rightarrow 13$
6517 independent reflections	$l = -19 \rightarrow 19$

Refinement

Refinement on F^2	$w = 1/[\sigma^2(F_o^2) + (0.0778P)^2 + 0.1431P]$ where $P = (F_o^2 + 2F_c^2)/3$
$R[F^2 > 2\sigma(F^2)] = 0.049$	$(\Delta/\sigma)_{max} = 0.001$
$wR(F^2) = 0.137$	$\Delta\rho_{max} = 0.30$ e Å^{-3}
$S = 1.10$	$\Delta\rho_{min} = -0.37$ e Å^{-3}
6512 reflections	
399 parameters	
H-atom parameters constrained	

Table 5
Hydrogen-bonding geometry (Å, °) for polymorph (II*b*).

D—H···A	D—H	H···A	D···A	D—H···A
N15—H15*B*···O18	0.88	1.99	2.6451 (17)	130
N25—H25*A*···O28	0.88	1.95	2.6069 (19)	131
N25—H25*B*···O13	0.88	2.19	3.0586 (17)	170
C12—H12*A*···O18^{i}	0.99	2.27	3.221 (2)	161

Symmetry code: (i) $x-1, y, z$.

Compound (III)

Crystal data

$C_{17}H_{12}F_3NO_3$	$Z = 4$
$M_r = 335.28$	$D_x = 1.544$ Mg m^{-3}
Triclinic, $P\overline{1}$	Mo $K\alpha$ radiation
$a = 7.3420$ (2) Å	Cell parameters from 6611 reflections
$b = 10.9241$ (3) Å	$\theta = 3.0$–$27.6°$
$c = 18.7176$ (5) Å	$\mu = 0.13$ mm^{-1}
$\alpha = 85.0180$ (11)°	$T = 120$ (2) K
$\beta = 83.2280$ (14)°	Block, red
$\gamma = 75.8180$ (14)°	0.60 × 0.60 × 0.50 mm
$V = 1442.71$ (7) Å^3	

Data collection

Nonius KappaCCD area-detector diffractometer	6611 independent reflections
φ and ω scans	4510 reflections with $I > 2\sigma(I)$
Absorption correction: multi-scan (*SADABS*; Sheldrick, 2003)	$R_{int} = 0.038$
$T_{min} = 0.920$, $T_{max} = 0.937$	$\theta_{max} = 27.6°$
20 172 measured reflections	$h = -9 \rightarrow 6$
	$k = -14 \rightarrow 13$
	$l = -24 \rightarrow 24$

Refinement

Refinement on F^2	$w = 1/[\sigma^2(F_o^2) + (0.0874P)^2 + 0.3568P]$ where $P = (F_o^2 + 2F_c^2)/3$
$R[F^2 > 2\sigma(F^2)] = 0.052$	$(\Delta/\sigma)_{max} < 0.001$
$wR(F^2) = 0.157$	$\Delta\rho_{max} = 0.77$ e Å^{-3}
$S = 1.04$	$\Delta\rho_{min} = -0.52$ e Å^{-3}
6611 reflections	
433 parameters	
H-atom parameters constrained	

Table 6
Hydrogen-bonding geometry (Å, °) for (III).

D—H···A	D—H	H···A	D···A	D—H···A
N15—H15*A*···O18	0.96	1.91	2.637 (2)	131
N15—H15*B*···O11^{i}	0.96	2.26	3.161 (2)	156
N25—H25*A*···O28	0.96	1.91	2.662 (2)	134
N25—H25*B*···O21^{i}	0.96	2.09	3.024 (2)	165

Symmetry code: (i) $x-1, y, z$.

For (I) and (II*a*), the space groups $P2_1/n$ and $P2_1/c$, respectively, were uniquely determined from the systematic absences. Crystals of (II*b*) and (III) are triclinic, and the space group $P\overline{1}$ was selected and then confirmed by the structure analysis. All H atoms were located from difference maps and subsequently treated as riding atoms, with C—H = 0.95 (CH), 0.98 (CH_3) or 0.99 Å (CH_2) and N—H = 0.96 Å, and with U_{iso}(H) = 1.2U_{eq}(C,N), or 1.5U_{eq}(C) for the methyl groups. In compound (III), the highest residual peak (0.77 e Å^{-3}) is 1.26 Å from F141 and the deepest hole (−0.52 e Å^{-3}) is 0.97 Å from F141. Careful inspection of electron-density maps indicated some libration of the CF_3 groups about the adjacent C—C bonds, but gave no grounds for modelling these groups with more than three F-atom sites per group.

For all four compounds, data collection: *COLLECT* (Nonius, 1998). For compound (I), cell refinement: *DIRAX*/*LSQ* (Duisenberg *et al.*, 2000); data reduction: *EvalCCD* (Duisenberg *et al.*, 2003); program(s) used to solve structure: *SIR*97 (Altomare *et al.*, 1999); program(s) used to refine structure: *OSCAIL* (McArdle, 2003) and *SHELXL*97 (Sheldrick, 1997). For compounds (II*a*) and (III), cell refinement: *DENZO* (Otwinowski & Minor, 1997) and *COLLECT*; data reduction: *DENZO* and *COLLECT*; program(s) used to solve structure: *SHELXS*97 (Sheldrick, 1997); program(s) used to refine structure: *SHELXL*97. For compound (II*b*), cell refinement: *DENZO* and *COLLECT*; data reduction: *DENZO* and *COLLECT*; program(s) used to solve structure: *OSCAIL* and *SHELXS*97;

program(s) used to refine structure: *OSCAIL* and *SHELXL*97. For all four compounds, molecular graphics: *PLATON* (Spek, 2003); software used to prepare material for publication: *SHELXL*97 and *PRPKAPPA* (Ferguson, 1999).

The X-ray data for compounds (II) and (III) were collected at the EPSRC X-ray Crystallographic Service, University of Southampton, England; the authors thank the staff for all their help and advice. JNL thanks NCR Self-Service, Dundee, for grants which have provided computing facilities for this work. RA thanks 'Fundación para la Promoción de la Investigación y la Tecnología (Banco de la República)' and Universidad del Valle for financial support. PC thanks COLCIENCIAS for a doctoral fellowship. JC and MN thank Consejería de Educación (Junta de Andalucía, Spain) for financial support.

Supplementary data for this paper are available from the IUCr electronic archives (Reference: SK1762). Services for accessing these data are described at the back of the journal.

References

Allen, F. H., Kennard, O., Watson, D. G., Brammer, L., Orpen, A. G. & Taylor, R. (1987). *J. Chem. Soc. Perkin Trans.* 2, pp. S1–19.
Altomare, A., Burla, M. C., Camalli, M., Cascarano, G. L., Giacovazzo, C., Guagliardi, A., Moliterni, A. G. G., Polidori, G. & Spagna, R. (1999). *J. Appl. Cryst.* **32**, 115–119.
Bernstein, J., Davis, R. E., Shimoni, L. & Chang, N.-L. (1995). *Angew. Chem. Int. Ed. Engl.* **34**, 1555–1573.
Burger, A. & Ramberger, R. (1979). *Mikrochim. Acta*, **2**, 259–271.
Cremer, D. & Pople, J. A. (1975). *J. Am. Chem. Soc.* **97**, 1354–1358.
Donnelly, J. A. & Farell, D. F. (1990). *Tetrahedron*, **46**, 885–894.
Duisenberg, A. J. M., Hooft, R. W. W., Schreurs, A. M. M. & Kroon, J. (2000). *J. Appl. Cryst.* **33**, 893–898.
Duisenberg, A. J. M., Kroon-Batenburg, L. M. J. & Schreurs, A. M. M. (2003). *J. Appl. Cryst.* **36**, 220–229.
Ferguson, G. (1999). *PRPKAPPA*. University of Guelph, Canada.
Kurasawa, Y., Tsuruoka, A., Rikiishi, N., Fujiwara, N., Okamoto, Y. & Kim, H. S. (2002). *J. Heterocycl. Chem.* **37**, 791–798.
Low, J. N., Cobo, J., Nogueras, M., Sánchez, A., Albornoz, A. & Abonia, R. (2002). *Acta Cryst.* C**58**, o42–o45.
McArdle, P. (2003). *OSCAIL for Windows*. Version 10. Crystallography Centre, Chemistry Department, NUI Galway, Ireland.
Nonius (1998). *COLLECT*. Nonius BV, Delft, The Netherlands.
Otwinowski, Z. & Minor, W. (1997). *Methods in Enzymology*, Vol. 276, *Macromolecular Crystallography*, Part A, edited by C. W. Carter Jr & R. M. Sweet, pp. 307–326. New York: Academic Press.
Prager, R. & Thredgold, M. (1968). *Aust. J. Chem.* **21**, 229–241.
Sheldrick, G. M. (1997). *SHELXS*97 and *SHELXL*97. University of Göttingen, Germany.
Sheldrick, G. M. (2003). *SADABS*. Version 2.10. University of Göttingen, Germany.
Spek, A. L. (2003). *J. Appl. Cryst.* **36**, 3–17.